

MODELLING AND SIMULATION OF THE RHEOLOGY OF BULK MOULDING COMPOUNDS (BMC) DURING MOULD FILLING

Pierre J.J. Dumont¹, Olivier Guiraud², Laurent Orgéas², Thai-Hung Le², Denis Favier²

¹Laboratoire de Génie des Procédés Papetiers (LGP2), CNRS-INPG-EFPG, 461 rue de la Papeterie, BP 65, 38402 Saint-Martin-d'Hères cedex, France

²Laboratoire Sols-Solides-Structures-Risques (3SR), CNRS, Universités de Grenoble (INPG-UJF), BP 53, 38041 Grenoble cedex 9, France
pierre.dumont@efpg.inpg.fr

KEYWORDS: Fibrous concentrated suspension, BMC, rheology, constitutive modelling, FE simulation.

ABSTRACT

Bulk Moulding Compounds (BMC's) are thermoset polymer composites widely used in electric and automotive industries. They are processed by injection or compression moulding. Unfortunately, their rheology during mould filling is not well known due to scarce studies, which hinders the optimization of process conditions. Thereby, our objective is to determine experimentally the main features of the BMC's rheology. For that purpose, homogeneous simple and plane strain compression tests are performed. The resulting data are used to build a 3D tensorial model of the BMC rheology, which is implemented in a FE code. Finally, numerical simulations are compared with experiments achieved with rather complex flow situations.

1. INTRODUCTION

Bulk Moulding Compounds (BMC) are composite materials that are made of a pasty filled thermoset polymer matrix reinforced by entangled short glass fibres. They are widely used by the electric industry to produce small components having good surface appearance and complex shapes. Their processing route can be split into three main phases: (1) the compounding phase, which consists in mixing uncured polyester resin, mineral fillers, glass-fibre bundles and other additives, (2) the injection moulding phase (1 - 10 s) during which these compounds are forced by an injection screw to fill a hot mould (150°C), (3) the resin cure within the hot mould (60 - 180 s).

Few studies concern the rheology of BMC's during the injection moulding phase. [1] have shown that BMC's flow inside the mould associates shear and elongational deformation modes. [2-3] have shown that BMC's follow a temperature-dependent shear-thinning behaviour. However, in these studies, BMC's were subjected to heterogenous deformation modes: it means that a priori constitutive assumptions had to be used to build constitutive models from these studies. Moreover, the dimensions of the rheometers were not large enough compared with the typical length of glass fibres contained in BMC and this might increase the variability of experimental results and hide some experimental trends [4]. In order to tackle these different problems, simple compression experiments were recently performed in [5] using large samples. Results permitted to propose a non-linear viscoelastic model for the rheology of the studied BMC's, accounting particularly for a strain-hardening behaviour. However this model is only one-dimensional. Therefore, it has to be improved to build a 3D tensorial form in order to use it for performing simulations of encountered flow situations in moulds.

Here, samples were deformed under lubricated and homogeneous simple compression and plane strain compression modes at constant axial strain rates. All compression data were corrected to account for the influence of the lubrication layers put between the samples and the plates of the used rheometers. Experimental results emphasize the

influence of the imposed strain rate and strain, on the BMC rheology. Results are used to build a simple 3D non-linear viscous model. This model is implemented into a finite element simulation software. Then predictions of this model are compared with some experimental compression results obtained using a mould having in-plane cylindrical obstacles.

2. MATERIALS AND EXPERIMENTAL PROCEDURE

2.1. Materials

Tested BMC materials were supplied by Compositec (le Bourget-du-Lac, France). They are made up of polyester resin (35.25 wt%), zinc stearate (2.65% wt), moulding agents (8.8 wt%), filled with alumina (53.3 wt%) and reinforced with bundles of glass fibres (length 15 mm, 200 fibres of 13.7 μm in diameter) at a mass fraction $f = 20\%$. In order to account for the modifications entailed by the flow through an injection screw on the microstructure of the BMC compounds during the industrial process, tested BMC's were preliminary poured into an injection screw and taken at its exhaust.

2.2. Experimental procedure and apparatus

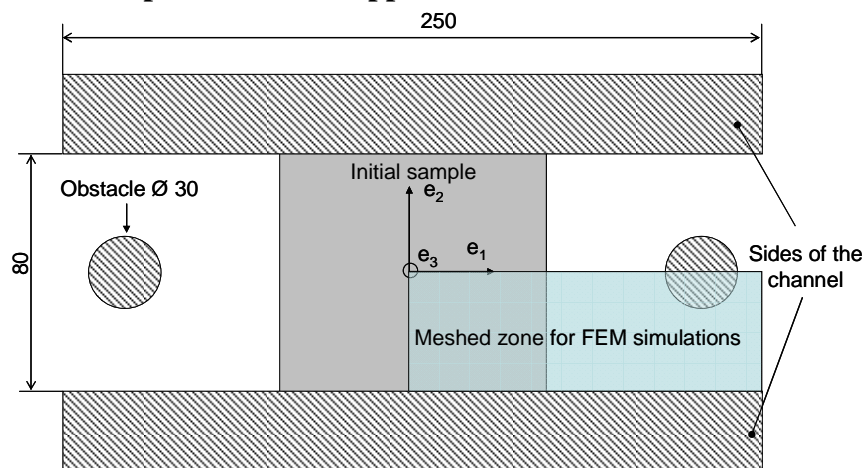


Figure 1: Scheme of the top view of the channel compression mould with in-plane obstacles.

Then homogeneous simple and plane strain (channel) compression tests were performed using a specially developed transparent rheometer, which dimensions are compatible with the length of bundles (see [4]). This rheometer was mounted on a MTS mechanical testing machine (20 kN, cross-head velocity 8 mm s^{-1}). For simple compression tests, cylindrical samples having a diameter $D_0 = 70$ mm or $D_0 = 110$ mm and an initial height $h_0 = 20$ mm were used. For plane strain compression tests, rectangular samples of dimensions $L_0 \times l_0 \times h_0 = 80 \times 80 \times 20$ mm³ and $L_0 \times l_0 \times h_0 = 160 \times 80 \times 20$ mm³ were used. Each tested sample was lubricated by coating it with a thin layer of silicone grease as well as the plates of the rheometer in contact with it in order to perform homogeneous flow kinematics [4, 5]. Compression tests were performed at various constant axial strain rates $D_{33} = 10^{-2}$; 10^{-1} and $3 \cdot 10^{-1}$ s^{-1} at constant room temperature ($T = 296$ K). For both types of tests the axial force F_3 was measured, whereas, for plane strain compression tests, the lateral force F_2 exerted on the sides of the channel was measured. A third type of compression test was also carried out, i.e. compression through a channel with in-plane cylindrical obstacles (see figure 1) at different constant axial strain rates $D_{33} = 10^{-2}$; 10^{-1} and $3 \cdot 10^{-1}$ s^{-1} . During the tests, the current height h of the samples was also recorded. It was then possible to calculate respectively the axial Hencky strain and the axial strain rate:

$$\varepsilon_{33} = \ln \frac{h}{h_0}, \quad D_{33} = \frac{\dot{h}}{h}. \quad (1)$$

Assuming that BMC materials are incompressible, the average axial stress is calculated in the case of simple compression tests as follows:

$$\bar{\sigma}_{33sc} = \frac{4F_3 h}{\pi D_0^2 h_0}, \quad (2)$$

and in the case of plane strain compression tests, the average axial stress and the average lateral stress are respectively:

$$\bar{\sigma}_{33ps} = \frac{F_3 h}{l_0 L_0 h_0}, \quad \bar{\sigma}_{22ps} = \frac{F_2}{L_0 h_0}. \quad (3)$$

3. EXPERIMENTAL RESULTS

3.1. General aspect of the stress-strain curves

Figure 2 gives the general aspect of the evolution of the average axial compression stress $\bar{\sigma}_{33sc}$ with respect to the axial strain ε_{33} for two different initial diameters $D_0 = 70$ and 110 mm.

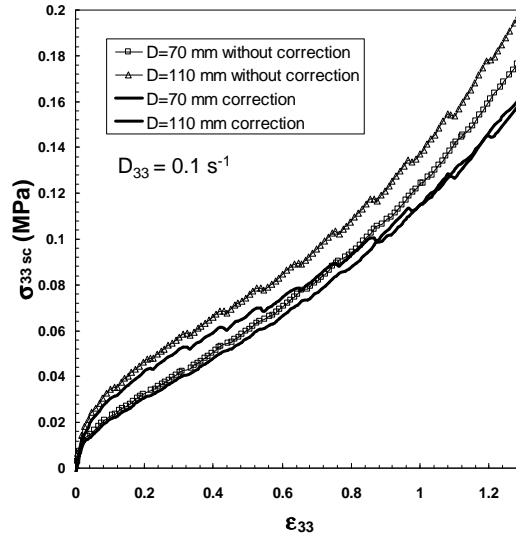


Figure 2: Triangles represent the evolution of the average axial stress $\bar{\sigma}_{33sc}$ with respect to the axial strain ε_{33} measured in the case of simple compression tests for two samples of BMC having different diameters, lines represent the corrected axial stress σ_{33sc} accounting for hydrodynamic friction coefficient ($f = 20\%$, $D_{33} = 10^{-1} \text{ s}^{-1}$, $D_0 = 70$ mm or 110 mm).

As it can be seen on these figures, there is an influence of the diameter of tested samples on the measured stress levels: the higher the diameter, the higher the measured stresses.

Similar tendencies are obtained for measurements of the axial and lateral average stresses $\bar{\sigma}_{33ps}$ and $\bar{\sigma}_{22ps}$ in cases of plane stress compression experiments: there is an influence of the lengths of the tested samples on the measurements. In previous experiments, this effect of the dimensions of the samples was attributed to the shearing of the thin layer of the silicone lubricant during the flow. A method has been proposed

in [5] in order to correct the stress-strain curves in the cases of simple compression tests accounting for a hydrodynamic friction coefficient (see the result of this correction on figure 2). The same type of corrections as in [5] has been performed here for plane strain compression experiments too. Details of the developments of the correction term in cases of plane strain compression are not presented but are very similar to those carried out for simple compression. All results presented in the next parts are based on corrected stress measurements.

3.2. Influence of strain rates

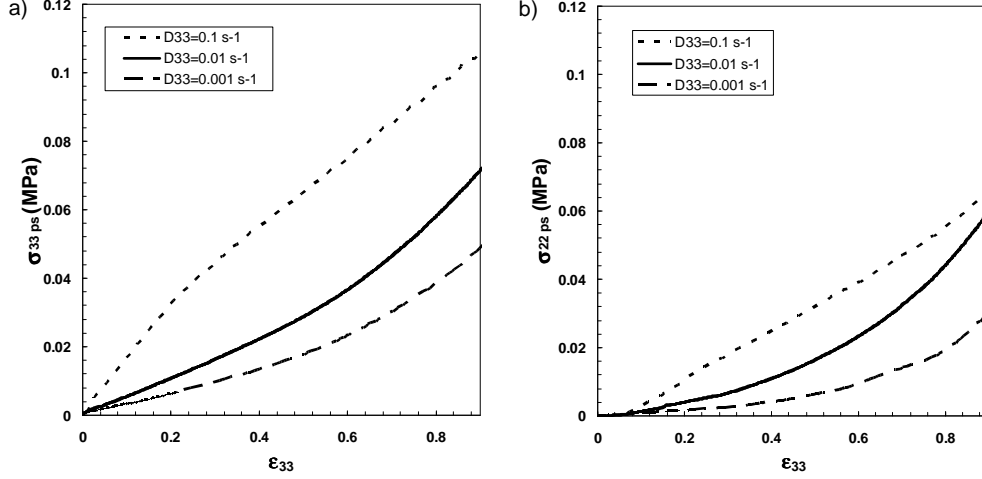


Figure 3: Evolution of a) the axial stress σ_{33ps} and b) the lateral stress σ_{22ps} with respect to the axial strain for three different strain rates: $D_{33} = 10^{-1}$, 10^{-2} and 10^{-3} s^{-1} ($f = 20\%$).

Figure 3 shows the evolution of the axial and lateral stresses for plane strain compression experiments. As evident from this figure there is a large impact of the axial strain rate D_{33} on the recorded stress levels. Similar observations were made in cases of simple compression experiments. This reveals the pronounced viscous behaviour of the tested BMC's.

Figures 4a represents the influence of the axial strain rate D_{33} on the axial stress σ_{33sc} measured at two different axial strains $\epsilon_{33} = 0.2$ and 0.8 . In the same way, figure 4b (resp. 4c) illustrates the influence of the axial strain rate D_{33} on the axial (resp. lateral) stress σ_{33ps} (resp. σ_{22ps}). It can be noticed that the evolutions of these stresses can be fitted using power-law functions of the axial strain rate D_{33} :

$$\sigma_{33sc} = \eta_{sc3} D_{33}^{n_{sc}}, \quad (4)$$

$$\sigma_{33ps} = \eta_{ps3} D_{33}^{n_{ps3}}, \quad (5)$$

$$\sigma_{22ps} = \eta_{ps2} D_{33}^{n_{ps2}}, \quad (6)$$

where $n_{sc} = 0.41$ and 0.35 ($n_{ps3} = 0.34$ and 0.22 ; $n_{ps2} = 0.46$ and 0.25) are strain rate sensitivities and $\eta_{sc3} = 0.10 \text{ MPa s}^{-n}$ and 0.22 MPa s^{-n} are some “viscosities” ($\eta_{ps3} = 0.09 \text{ MPa s}^{-n}$ and 0.22 MPa s^{-n} ; $\eta_{ps2} = 0.05 \text{ MPa s}^{-n}$ and 0.18 MPa s^{-n}) measured at $\epsilon_{33} = 0.2$ and 0.8 , respectively.

It is interesting to notice that the strain rate sensitivity coefficients decrease when increasing the axial strain ϵ_{33} . Increasing the axial strain has also for effect to increase the “viscosities” η_{sc3} , η_{ps3} and η_{ps2} showing thus a strain hardening effect during the deformation of the BMC materials.

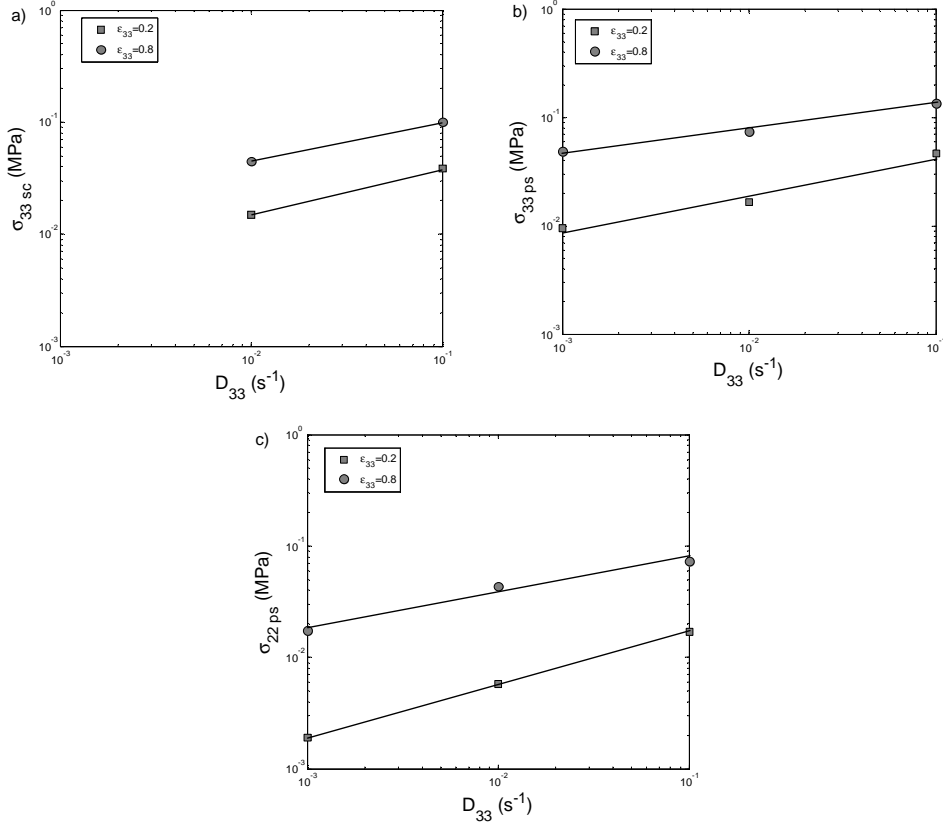


Figure 4: Evolution of a) the axial stress σ_{33sc} with respect to the axial strain rate D_{33} in cases of simple compression experiments of b) the axial stress σ_{33ps} and c) the lateral stress σ_{22ps} in cases of plane strain compression experiments at different levels of axial strain ϵ_{33} ($f = 20\%$).

4. TENSORIAL RHEOLOGICAL MODEL

4.1. Formulation

On the basis of the previous experimental results, a 3D tensorial model is proposed for the rheology of BMC's. They are seen as forming a one-phase and homogeneous medium from a macroscopic point of view. Moreover, they are considered as being incompressible materials, so that

$$I_D = \underline{\underline{\mathbf{D}}}: \underline{\underline{\delta}} = 0, \quad (7)$$

where $\underline{\underline{\mathbf{D}}}$ is the strain rate tensor, $\underline{\underline{\mathbf{D}}} = \frac{1}{2}(\underline{\underline{\text{grad}}}\ \underline{\underline{\mathbf{v}}} + {}^t\underline{\underline{\text{grad}}}\ \underline{\underline{\mathbf{v}}})$, $\underline{\underline{\mathbf{v}}}$ is the velocity field, $\underline{\underline{\delta}}$ is the unit tensor and I_D is the first invariant of $\underline{\underline{\mathbf{D}}}$. Therefore, the stress tensor is split into two parts:

$$\underline{\underline{\sigma}} = -p\underline{\underline{\delta}} + \underline{\underline{\sigma}}^v, \quad (8)$$

where p is an arbitrary pressure, $\underline{\underline{\sigma}}^v$ is the viscous part of the stress tensor. This latter is assumed to derive from a viscous potential Ω with respect to the strain rate tensor $\underline{\underline{\mathbf{D}}}$. This potential has to be a positive and convex function, with a gradient equal to zero when $\underline{\underline{\mathbf{D}}} = \underline{\underline{\mathbf{0}}}$. We further assume that this potential can be written using an equivalent strain rate D_{eq} , which is a scalar function of the strain rate tensor $\underline{\underline{\mathbf{D}}}$:

$$\underline{\underline{\Omega}} = \underline{\underline{\Omega}}(D_{eq}(\underline{\underline{\mathbf{D}}})) . \quad (9)$$

Then the viscous part $\underline{\underline{\sigma}}^v$ writes:

$$\underline{\underline{\sigma}}^v = \frac{\partial \underline{\underline{\Omega}}}{\partial \underline{\underline{\mathbf{D}}}} = \frac{\partial \underline{\underline{\Omega}}}{\partial D_{eq}} \frac{\partial D_{eq}}{\partial \underline{\underline{\mathbf{D}}}} = \sigma_{eq} \frac{\partial D_{eq}}{\partial \underline{\underline{\mathbf{D}}}} , \quad (10)$$

where σ_{eq} is the equivalent stress. Accounting for the strain-hardening and non-linear viscous effects, which are experimentally observed, this term is written as follows:

$$\sigma_{eq} = \eta D_{eq}^n \text{ with } \eta = \eta_{0eq} \exp(k \varepsilon_{eq}) , \quad (11)$$

where η_{0eq} is an equivalent viscosity of BMC's, ε_{eq} an equivalent strain, k is a strain-hardening parameter and n the strain-rate sensitivity.

Assuming that BMC's are isotropic materials, D_{eq} is given by the following equation:

$$D_{eq} = \sqrt{\frac{2}{3} \underline{\underline{\mathbf{D}}} : \underline{\underline{\mathbf{D}}}} \quad (12)$$

and similarly ε_{eq} is given by

$$\varepsilon_{eq} = \sqrt{\frac{2}{3} \underline{\underline{\boldsymbol{\varepsilon}}} : \underline{\underline{\boldsymbol{\varepsilon}}}} , \quad (13)$$

where $\underline{\underline{\boldsymbol{\varepsilon}}}$ is the Hencky strain tensor, i.e. $\underline{\underline{\boldsymbol{\varepsilon}}} = \int_0^t \underline{\underline{\mathbf{D}}} dt$, t being the time.

Then, the viscous stress tensor can be written:

$$\underline{\underline{\sigma}}^v = \frac{2}{3} \eta_{0eq} \exp(k \varepsilon_{eq}) D_{eq}^{n-1} \underline{\underline{\mathbf{D}}} . \quad (14)$$

4.2. Determination of model's parameters

Just three parameters have to be determined in the previous model: η_{0eq} , k and n . This has been done by considering the complete set of experimental results gained in simple compression and plane strain compression experiments. The following set of parameters was determined for the model in the range of tested strains and strain rates:

$$\eta_{0eq} = 0.05 \text{ MPa s}, \quad k = 1.3, \quad n = -0.19 \varepsilon_{eq} + 0.4. \quad (15)$$

Figure 6 shows a comparison between the predictions of the model and the experimental data where the evolution of the equivalent stress σ_{eq} with respect to the equivalent strain ε_{eq} has been reported for all tested equivalent strain rates D_{eq} . It can be noticed that the model fits rather well the experimental data whatever the considered flow kinematics. Of course, experimental and model curves differ at their beginnings due to the fact that the very simple proposed model cannot account for viscoelastic effects on the rheology of BMC's.

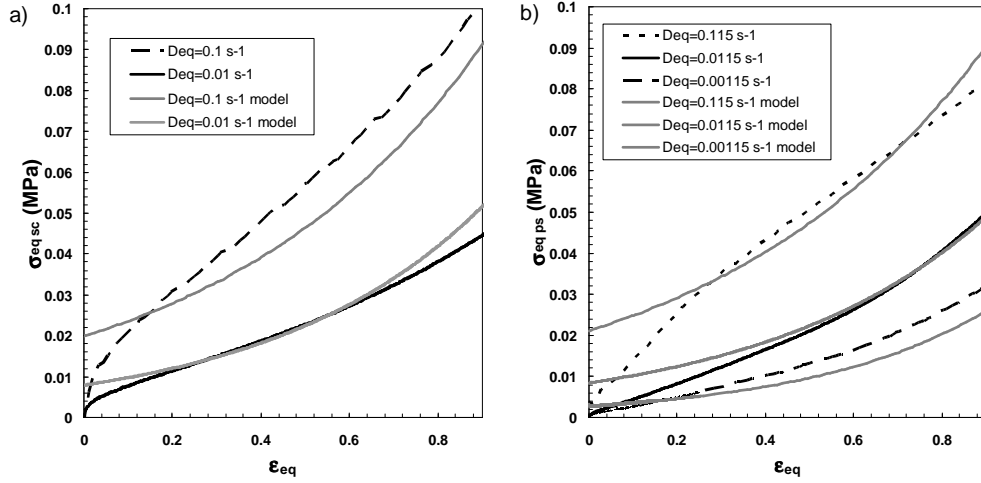


Figure 5: Comparison between experimental results and model predictions the evolution for a) simple compression and for b) plane strain compression ($f = 20\%$).

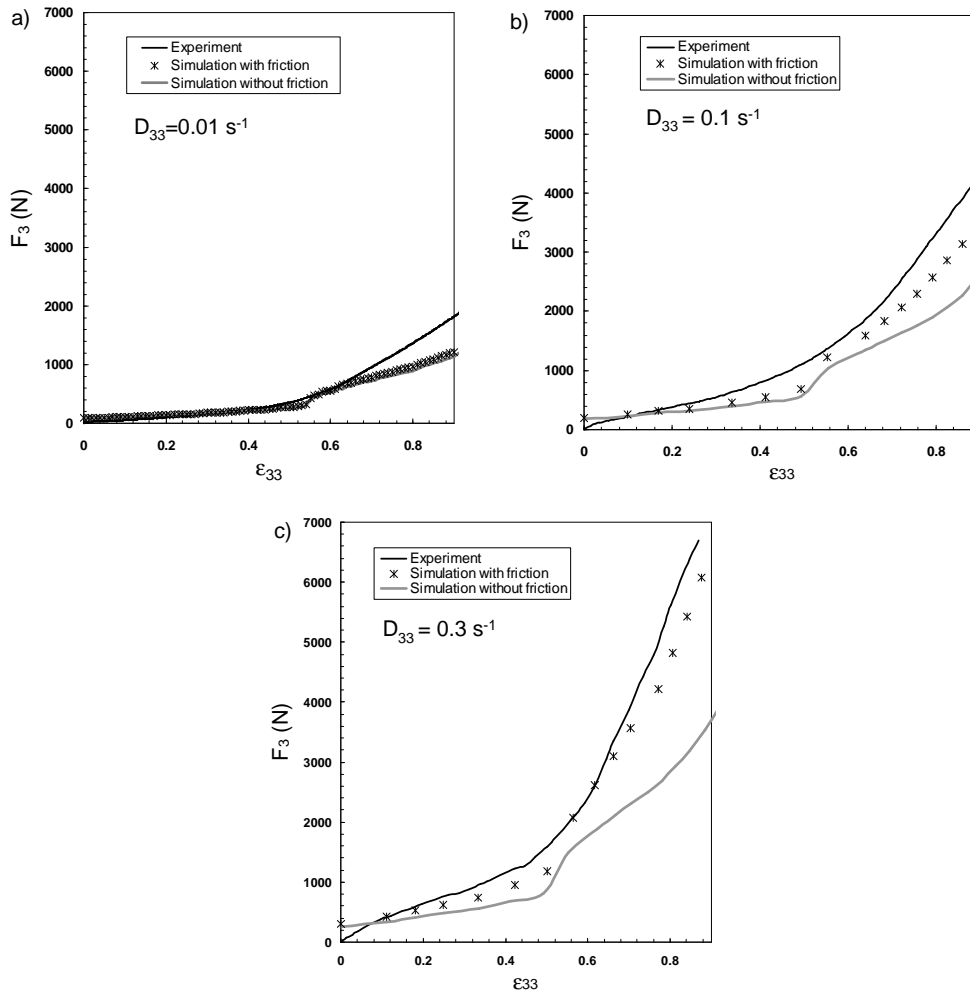


Figure 7: Comparison between the experimental and simulated evolutions of the axial force F_3 during compression experiments with channel mould having in-plane obstacles ($f = 20\%$). Two simulation cases are considered: with and without hydrodynamic friction effects.

4.2. FE simulation: comparison between model predictions and experiments

The as-determined model has been implemented into a finite element software specially designed to predict the flow behaviour of materials such as Sheet Moulding Compounds (SMC), Glass Mat Thermoplastics (GMT) (see [6-7]) and now BMC.

Basically, a plug flow assumption is made for the flow of the compounds inside the mould, but hydrodynamic friction effects having a similar form to that used to correct stress measurements can also be accounted for, if necessary. First simulations have checked that the implemented model gives similar results to its analytical version in cases of simple and plane strain compression simulations. Second simulations have permitted to calculate the time-evolution of the axial force F_3 in the case of compression carried out using the mould with in-plane obstacles (see its geometry on figure 1). Results given in figure 6 for different axial strain rates $D_{33} = 0.01; 0.1$ and 0.3 s^{-1} show that the simulation gives rather good results compared with the experimental observations. Best results are obtained when accounting for a friction effect between the mould and the BMC sample.

6. CONCLUSION

In this study, the rheological behaviour of BMC materials has been characterized using homogeneous simple and plane strain compression experiments. All stress measurements have been corrected accounting for the effect of the shearing of the lubricating silicone grease layer. Results show that the tested BMC's exhibit a non-linear viscous behaviour with a strain hardening effect. These different features have been used to build a 3D tensorial rheological model for the BMC's. This model has been implemented into a finite element software. This has permitted to show that there is a rather good agreement between the predictions of the model and some experimental results obtained in cases of rather complex flow situations. It has to be noticed that the best agreement has been obtained when accounting for the friction effect at the BMC / mould interfaces.

ACKNOWLEDGEMENTS

The authors would like to thank Compositec (Y. Gardet) for supplying BMC materials. O. Guiraud would like to thank the Région Rhône-Alpes (France) and the cluster Plastipolis for their support to his work through the grant they provide.

REFERENCES

1. Lafranche E, Menio S, Guegan M-L, Krawczak P, « Étude expérimentale des mécanismes d'écoulement dans le moulage par injection des BMC. » *Rev. Compos. Mater. Av.*, Vol. 12, pp. 461–475, 2002.
2. Blanc R., Agassant J.F., Vincent M., “Injection molding of unsaturated polyester compounds”, *Polym. Eng. Sci.*, Vol. 32, No 19, pp. 1440-1450, 1992.
3. Kenny J., Opalicki M., “Processing of short fibre/thermosetting matrix composites”, *Composites Part A*, Vol. 27A, No 3, pp. 229-240, 1996.
4. Dumont P., Orgéas L., Le Corre S., Favier D., “Anisotropic viscous behavior of Sheet Molding Compounds (SMC) during compression molding”, *International Journal of Plasticity*, Vol. 19, No. 5, pp. 625-646, 2003.
5. Orgéas L., Dumont P.J.J., Le T.H., Favier D., “Lubricated compression of BMC, a concentrated and fibre-reinforced granular polymer suspension”, accessible on-line in *Rheol. Acta*, 2008.

6. Dumont P., Orgéas L., Favier D., Pizette P., Venet C., “Compression of SMC: in-situ experiments, modelling and simulation”, *Composites: Part A.*, Vol. 38, pp. 353-368, 2007.
7. Dumont P., Le Corre S., Orgéas L., Favier D., Gaborit C., Lory P., “Finite element implementation of a two-phase model for compression molding of composites”, *Euro. J. Comput. Mech.*, Vol. 14, pp. 885-902, 2005.